AMERICAN SOCIETY of
GENE & CELL
THERAPY

Therapeutic Targeting of AXL Receptor Tyrosine Kinase Inhibits Tumor Growth and Intraperitoneal Metastasis in Ovarian Cancer Models

Pinar Kanlikilicer,[1] Bulent Ozpolat,[1] Burcu Aslan,[1] Recep Bayraktar,[1] Nilgun Gurbuz,[1] Cristian Rodriguez-Aguayo,[1] Emine Bayraktar,[1] Merve Denizli,[1] Vianey Gonzalez-Villasana,[1] Cristina Ivan,[1] Ganesh L.R. Lokesh,[2] Paola Amero,[1] Silvia Catuogno,[3] Monika Haemmerle,[4] Sherry Yen-Yao Wu,[4] Rahul Mitra,[4] David G. Gorenstein,[2] David E. Volk,[2] Vittorio de Franciscis,[3] Anil K. Sood,[4,5] and Gabriel Lopez-Berestein[1,5]

[1]Department of Experimental Therapeutics, The University of Texas MD Anderson Cancer Center, Houston, TX 77030, USA; [2]Brown Foundation Institute of Molecular Medicine, McGovern Medical School, The University of Texas Health Science Center at Houston, Houston, TX 77030, USA; [3]Istituto di Endocrinologia ed Oncologia Sperimentale, CNR, 80131 Naples, Italy; [4]Department of Gynecologic Oncology and Reproductive Medicine, The University of Texas MD Anderson Cancer Center, Houston, TX 77030, USA; [5]Department of Cancer Biology, The University of Texas MD Anderson Cancer Center, Houston, TX 77030, USA

Despite substantial improvements in the treatment strategies, ovarian cancer is still the most lethal gynecological malignancy. Identification of drug treatable therapeutic targets and their safe and effective targeting is critical to improve patient survival in ovarian cancer. AXL receptor tyrosine kinase (RTK) has been proposed to be an important therapeutic target for metastatic and advanced-stage human ovarian cancer. We found that AXL-RTK expression is associated with significantly shorter patient survival based on the The Cancer Genome Atlas patient database. To target AXL-RTK, we developed a chemically modified serum nuclease-stable AXL aptamer (AXL-APTAMER), and we evaluated its in vitro and in vivo antitumor activity using in vitro assays as well as two intraperitoneal animal models. AXL-aptamer treatment inhibited the phosphorylation and the activity of AXL, impaired the migration and invasion ability of ovarian cancer cells, and led to the inhibition of tumor growth and number of intraperitoneal metastatic nodules, which was associated with the inhibition of AXL activity and angiogenesis in tumors. When combined with paclitaxel, in vivo systemic (intravenous [i.v.]) administration of AXL-aptamer treatment markedly enhanced the antitumor efficacy of paclitaxel in mice. Taken together, our data indicate that AXL-aptamers successfully target in vivo AXL-RTK and inhibit its AXL activity and tumor growth and progression, representing a promising strategy for the treatment of ovarian cancer.

INTRODUCTION

Ovarian cancer (OC) is the leading cause of gynecologic cancer-related deaths for women in the United States and throughout the world.[1] High-grade serous OC accounts for 70% of the OC cases and is associated with poor patient survival and clinical prognosis, and 5-year survival rate is about 29%–50%.[2] Surgery followed by chemotherapy is the principal treatment strategy for high-grade serous OC.[3] Although initial response to chemotherapy is high, most patients develop resistance and relapse. In addition to adverse and toxic effects, chemotherapy can cause complications related to intraperitoneal catheters.[4–6] Therefore, new treatment approaches are urgently needed to improve patient survival.

Tyrosine kinases are major targets for therapies because of their roles in the modulation of growth factor signaling and tumor metastasis.[7–9] The receptor tyrosine kinase AXL has been characterized as oncogenic because of its promotion of cancer cell survival, proliferation, invasion, and metastasis.[10–12] AXL knockdown was also shown to inhibit angiogenesis by impairing endothelial tube formation.[13] Upregulation of AXL expression has been reported in many cancers, including OC and cancers of the lung, prostate, breast, and pancreas.[10,11,14–16] AXL has been well identified as a therapeutic target in OC.[17–22] Rankin and colleagues showed that AXL is highly expressed in high-grade serous and metastatic ovarian tumors, but not in normal ovarian epithelium or tumor stroma.[23] Given the role of AXL as a prognostic marker for OC, inhibition of AXL in ovarian tumors holds a great therapeutic potential to render/slow cancer progression.

AXL inhibitors have been shown to inhibit oncogenic downstream signaling pathways, and they offer great therapeutic efficacy and sensitivity,[24,25] suggesting that inhibition of AXL is indeed an attractive strategy for OC patients. Several therapeutic approaches,

A

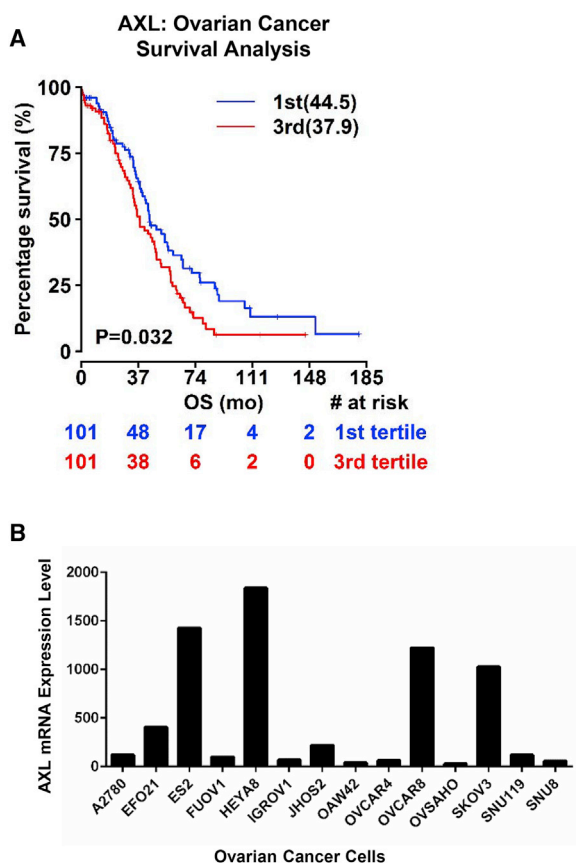**AXL: Ovarian Cancer Survival Analysis**

B

Figure 1. AXL Expression Is Associated with Poor Overall Patient Survival and a Bad Prognostic Factor in OC

(A) RNASeqv2 Level3 data were downloaded from the publicly available Cancer Genome Atlas Project for AXL in patients with ovarian serous cystadenocarcinoma (OV). Patient overall survival information was retrieved from cbioPortal. Overall survival rates significantly differ in low- and high-AXL expression. High AXL level is associated with shorter patient survival (n = 303, p < 0.032). (B) Analysis of Cancer Cell Line Encyclopedia (CCLE) database for AXL expression profile in OC cells. CCLE converted raw Affymetrix CEL files to a single value for each probeset using robust multi-array average (RMA) and quantile normalization. HeyA8 and SKOV3-IP1 cell are selected for further experiments based on the cell expression data.

including antibodies and small molecule inhibitors, have been used. Although targeted therapies have good toxicity profiles, it has been reported that patients who were treated with small molecular inhibitors, such as anti-EGFR, anti Her-2, and antiangiogeneic agents, developed severe toxicities.[26] The other targeted therapies, non-coding RNAs and aptamers, are emerging alternatives with potentially less toxic effects than current standard therapies.[22,27–30]

Aptamers, single-stranded small-sequence nucleic acids that can bind and inhibit their targets with high affinity and specificity, have emerged as a therapeutic strategy comparable to antibodies. They are easier to synthesize and more cost effective than antibodies, and they have negligible immunogenicity; easy manipula-

tion, manufacturing, and conjugation; and they can be chemically modified to enhance their nuclease resistance.

Our study showed that the chemically modified DNA aptamer was highly effective in inhibiting AXL in vivo and demonstrated significant reduction in antitumor/metastasis, further enhancing the efficacy of paclitaxel in OC tumor models.

RESULTS

AXL Overexpression Is Associated with Poor Survival in OC Patients

To determine the clinical significance of AXL expression, we analyzed The Cancer Genome Atlas (TCGA) database AXL mRNA expression with OC patient survival (Figure 1A). TCGA data analysis revealed that overexpression of AXL gene was correlated with poor survival in OC patients (p < 0.032). We also analyzed the Cancer Cell Line Encyclopedia (CCLE) database for AXL mRNA expression profile in 14 different OC cell lines (Figure 1B). AXL was highly expressed in most of the OC cell lines analyzed. HeyA8, OVCAR8, ES2, and SKOV3-IP1 are the top four cell lines with the highest AXL expression among the other OC cells (Figure 1B). Based on these data, we selected HeyA8 and SKOV3-IP1 for further in vitro and in vivo experiments.

AXL-APTAMER Is Stable and Binds to AXL with High Affinity

Given the role of fluoro- and monothiophosphate modifications on increased stability against nucleases, we synthesized a DNA aptamer that contained 2′-fluoro modifications on the pyrimidines as well as monothiophosphate modifications on selected nucleotides, using the RNA aptamer as the base sequence. The secondary structure of AXL-APTAMER was predicted by Mfold[31] software (Figure 2A). The Gibbs free energy of the folded aptamer was estimated to be −3.22 kcal/mol. The stability of the AXL-APTAMER in medium containing 80% human serum from 1 hr to 7 days was evaluated by denaturing PAGE (Figure 2B). AXL-APTAMER was found to be stable for up to 24 hr in 80% serum, indicating that AXL-APTAMER is able to provide resistance against nucleases for further therapeutic applications.

Furthermore, we incubated SKOV3-IP1 cells for 30 min with Cy3-labeled AXL-APTAMER (400 nM) to evaluate the localization of AXL-APTAMER in cells. After fixing the cells, we used immunofluorescence to visualize the localization. AXL-APTAMER was localized at the cell surface, whereas cells treated with a control aptamer displayed almost no signal (Figure 2C). A filter-binding assay used to generate binding data defined the dissociation constant of AXL-APTAMER as 130 nM (Figure 2D).

AXL-APTAMER Inhibits AXL Activity and Reduces OC Cell Proliferation In Vitro

We next determined whether the AXL signaling is inhibited by AXL-APTAMER treatment in OC cells. The level of phosphorylated AXL
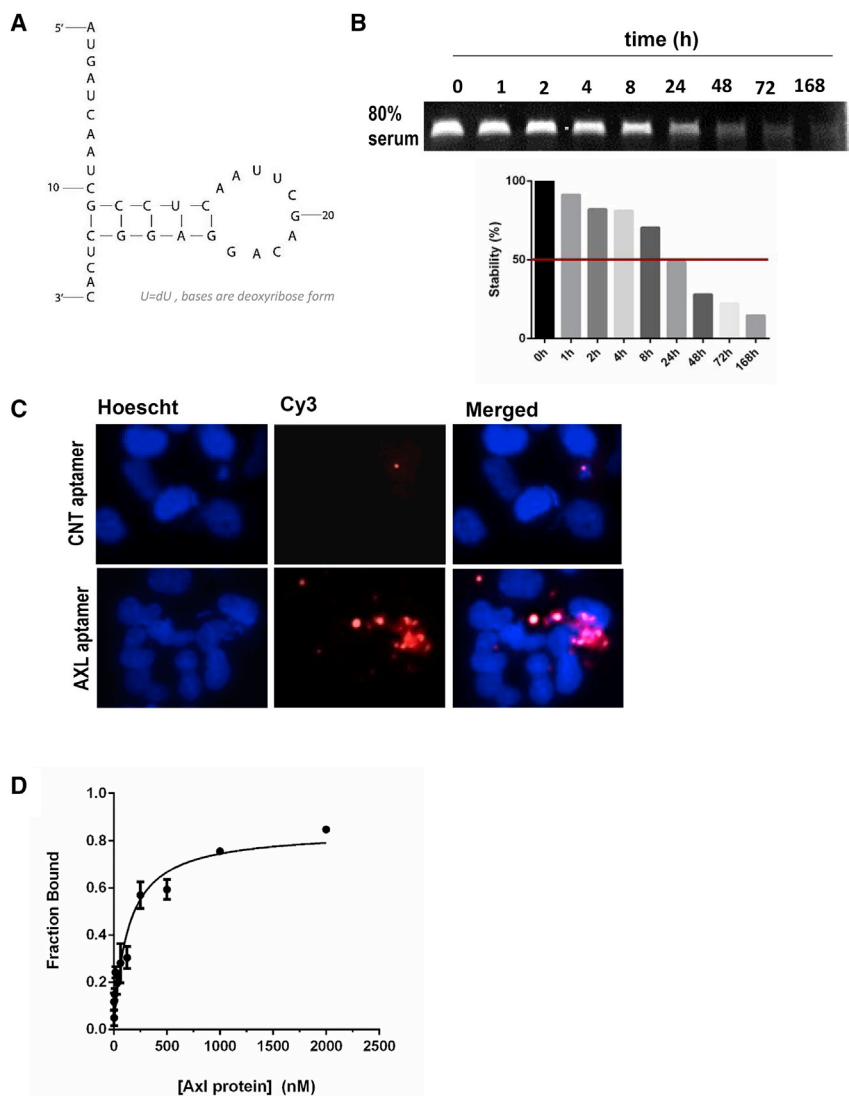
Figure 2. AXL-APTAMER Inhibits AXL Activation in OC Cells

(A) Secondary structure of AXL aptamer predicted by Mfold software. Gibbs free energy of the folded aptamer was calculated as −3.22 kcal/mol. All bases are deoxyribose form. (B) Stability of AXL-APTAMER in 80% serum. AXL-APTAMER is around 50% stable 24 hr in high-percentage (80%) serum. (C) Immunofluorescent images of Cy3-labeled AXL-APTAMER binding to cells. Hoescht was used to visualize nuclei. (D) Filter-binding assay was used to determine the affinity of AXL-APTAMER. Error bars represent mean values ± SEM.

(pAXL) was determined by western blot analysis in untreated and AXL-APTAMER-treated SKOV3-IP1 OC cells (Figure 3A). Treatment for 24 hr with the AXL-APTAMER (400 nM) reduced pAXL levels compared to control aptamer.

To elucidate the potential mechanism underlying the therapeutic activity of the AXL-APTAMER, we studied its effect on cell proliferation in vitro. SKOV3-IP1 and HeyA8 cells were treated with different concentrations of AXL-APTAMER for 24, 48, or 72 hr. Although we did not find any effect on cell proliferation with nanomolar concentration of AXL-APTAMER, 10 μM AXL-APTAMER treatment was found to reduce cell proliferation around 50% for SKOV3-IP1 and 20% for HeyA8 OC cells at 72 hr compared to control aptamer groups (Figure 3B). A concentration of 10 μM exhibited a time-dependent inhibition of SKOV3-IP1 and HeyA8 OC cell viability (Figure 3B). AXL-APTAMER exhibited more reduction in SKOV3-IP1 cell viability compared

to HeyA8 cells. We observed a dose-dependent inhibition of OC cell proliferation at 72 hr (Figure S1A).

Next, we investigated the effect of the AXL-APTAMER in combination with paclitaxel on in vitro OC cell proliferation by 3-(4,5-dimethylthiazol-2-yl)-5-(3-carboxy-methoxyphenyl)-2-(4-sulfophenyl)-2H-tetrazolium (MTS) cell proliferation assay. First IC_{50} values of paclitaxel were determined by treating HeyA8 and SKOV3-IP1 cells at varying doses (5, 10, 20, and 40 nM) of paclitaxel; 40 nM was identified as IC_{50} for both SKOV3-IP1 and HeyA8 cells (Figure S1B). Next, OC cells were grown to 70% confluency. After 24 hr, cells were treated with either AXL-APTAMER or the control aptamer (600 nM). Cells were then treated the next day with 40 nM paclitaxel. There was a slight but significant decrease in viability of these paclitaxel-sensitive cell lines. Paclitaxel combination inhibited HeyA8 and SKOV3-IP1 cell viability by 6.5% and 11.5% more, respectively, compared to control aptamer + paclitaxel at 48 hr (Figure S1C).

AXL-APTAMER Treatment Inhibits OC Migration and Invasion

Next, given the role of AXL downstream signaling in cancer cell metastasis, we investigated the potential role of AXL-APTAMER in inhibiting OC metastasis by wound healing and invasion assays. To this end, we first examined the effect of AXL-APTAMER on OC cell motility using the wound-healing assay, in which cell migration distances were monitored for 24 or 48 hr for SKOV3-IP1 and for 12 and 20 hr for HeyA8 OC cells. SKOV3-IP1 cells treated with AXL-APTAMER migrated shorter distances than cells treated with control aptamer (Figure 4A). Likewise, HeyA8 cells also migrated shorter distances than cells treated with control aptamer or cells without treatment (Figure 4B).
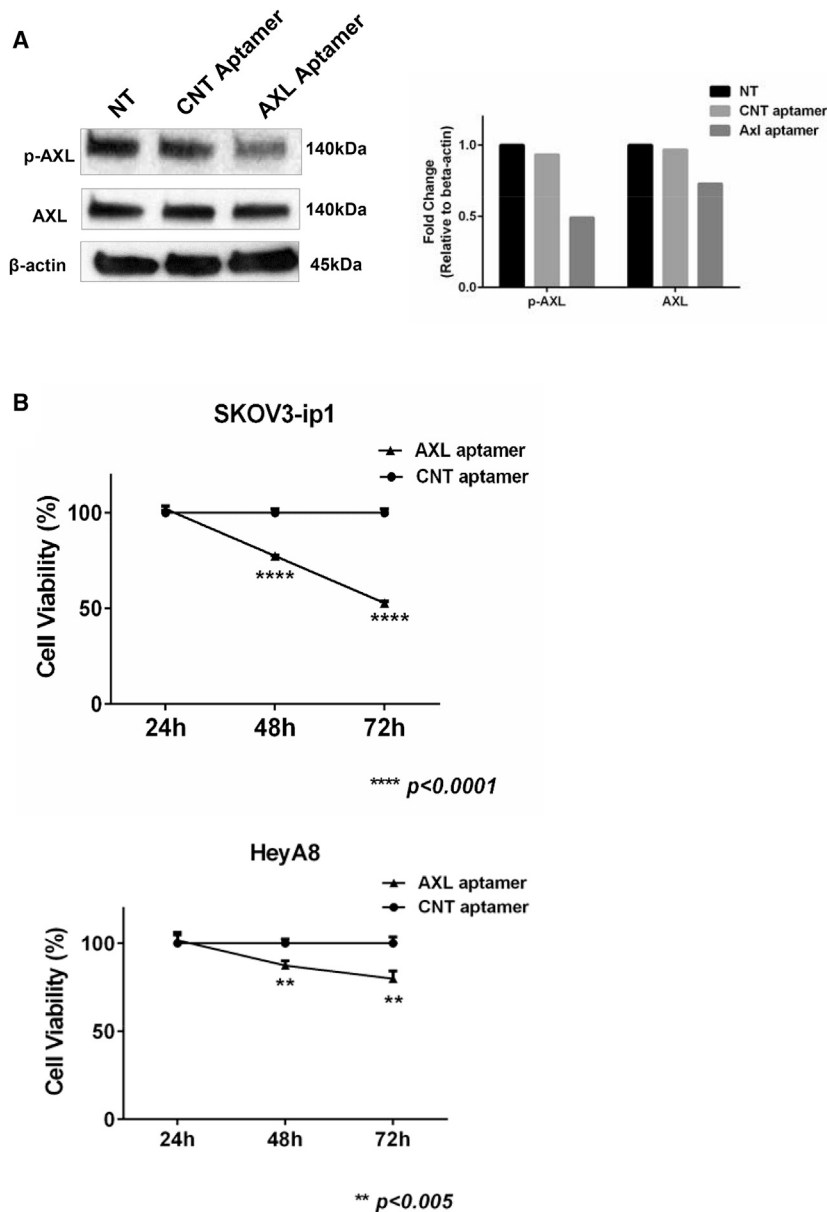
Figure 3. AXL-APTAMER Inhibits Downstream Signaling in OC Cells

(A) pAXL levels after AXL-APTAMER treatment detected by western blot alaysis. SKOV3-IP OC cells were treated for 3 hr with a control aptamer or AXL-APTAMER. Cell lysates were immunoprecipitated with pAXL. β-actin was used as the housekeeping protein. Quantification of the bands was performed using ImageJ software. (B) Cell viability was detected by MTS assay for SKOV3-IP1 and HeyA8 cell line using three different time points (24, 48, and 72 hr). All experiments were performed in six replicates, and the results were reported as the mean absorption ± SEM (**p < 0.001 and ****p < 0.0001).

Next, HeyA8 and SKOV3-IP1 OC cells were treated with either control aptamer or AXL-APTAMER, and their invasiveness was evaluated through the transwell matrigel invasion assay system (Figure 4C). Cells were harvested 24 hr after seeding and counted. Treatment with 400 nM AXL-APTAMER reduced percentages of invading HeyA8 and SKOV3-IP1 cells by approximately 80% and 60%, respectively, compared to control groups (Figure 4D).

To further elucidate the effects of the AXL-APTAMER on cancer metastasis, we analyzed invasion and migration markers in SKOV3-IP1 cells treated with AXL-APTAMER (400 nM). Immunoblotting showed that AXL-APTAMER reduced matrix metalloproteinase 2 (MMP2) and MMP1 expression compared to either no

treatment or control aptamer (Figure 4E). AXL-APTAMER treatment also reduced levels of phosphorylated focal adhesion kinase (p-FAK). Together, these findings demonstrate that AXL-APTAMER is effective in inhibiting the role of AXL in promoting cancer metastasis (Figure 4E).

AXL-APTAMER Treatment Inhibits OC Tumor Growth

To determine the effective in vivo therapeutic dose of the AXL-APTAMER that inhibited pAXL expression successfully, groups of mice (n = 3) bearing orthotopic ovarian tumors were injected (intravenously [i.v.] 1,600 pmol [0.6 mg/kg], 3,200 pmol [1.2 mg/kg], and 4,800 pmol [1.8 mg/kg]; days 0 and 2) with AXL-APTAMER in 100 μL PBS. Mice were euthanized on day 4 after injection, and tumors were collected and analyzed by immunoblotting to determine pAXL protein levels. We observed a dose-dependent pAXL down-modulation in this model (Figure 5A). The effective dose for further animal model studies was set at 4,800 pmol (1.8 mg/kg), three times a week.
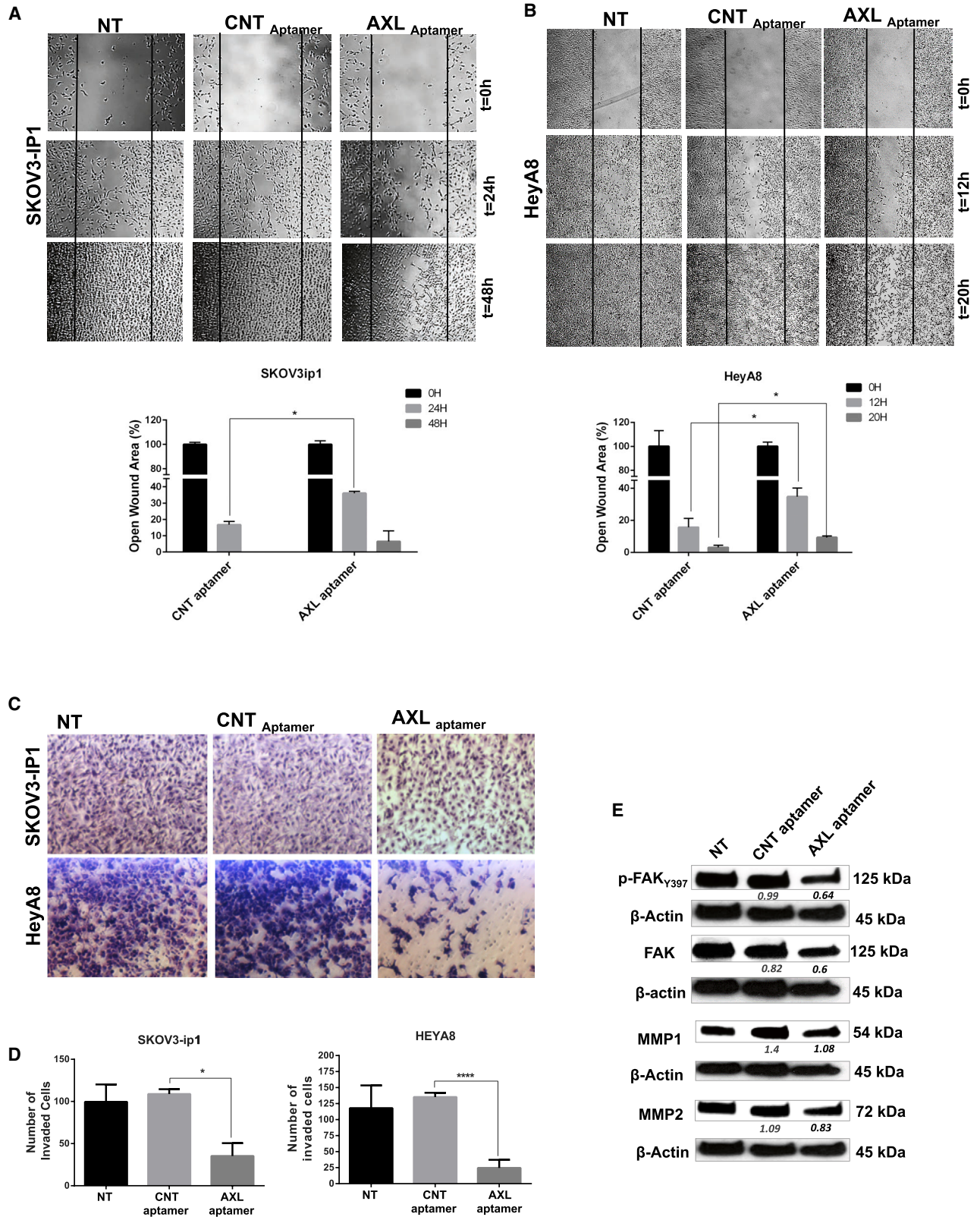
We next assessed the antitumor effects of AXL-APTAMER on two different (HeyA8 and metastatic SKOV3-IP1) OC orthotopic animal models. Given the potential role of targeting AXL oncoprotein in sensitizing cancer cells to chemotherapy, we also investigated the effects of AXL-APTAMER treatment in combination with paclitaxel in vivo. AXL-APTAMER was administered (1.8 mg/kg, three times a week) i.v. 2 weeks after tumor inoculation, and paclitaxel (3 mg/kg) was administered intraperitoneally once weekly.

We obtained our preliminary data on the HeyA8 animal model in which we used a small number of mice (n = 5) per group. We observed a striking inhibitory pattern for tumor weight and number of nodules for the AXL-APTAMER treatment group compared to the control aptamer treatment group, as well as for the paclitaxel combination groups (AXL-APTAMER + paclitaxel

A

B

SKOV3ip1

HeyA8

C

D

E

(legend on next page)

versus control aptamer + paclitaxel) (Figures S2A and S2B). None of the HeyA8 mouse groups showed significantly decreased body weight, indicating that the treatments were not toxic in this animal model (Figure S2C). No difference was observed between paclitaxel alone and control aptamer + paclitaxel groups in terms of tumor weight.

Because of the potential role of AXL in angiogenesis, we performed CD31 staining on frozen tumor samples to test the effect of AXL inhibition on tumor-associated angiogenesis. Immunohistochemistry analysis of tumors from control aptamer and AXL-APTAMER groups showed that there was a significant reduction in CD31-positive cells in the HeyA8 model (Figure S2D).

In the SKOV3-IP1 mouse model (n = 10), our results showed that AXL-APTAMER alone had a significant therapeutic effect, reducing mean tumor weight by 64.2% and mean number of tumor nodules by 45.2% compared to the group that received control aptamer (Figures 5B and 5C). The combination of AXL-APTAMER and paclitaxel reduced the tumor growth even further, resulting in 85% lower weight than in the group that received control + paclitaxel and 95% lower weight than in the group that received control aptamer alone. We observed no obvious toxic effects of AXL-APTAMER, which was evident from the non-significant differences in body weight among all mouse groups (Figure 5D).

Immunohistochemical analysis of tumor tissues from each group revealed that the SKOV3-IP1 tumor-bearing mice treated with AXL-APTAMER had significantly fewer pro-angiogenic CD31^{+} cells than the group treated with control aptamer (Figure 5E). Moreover, mice treated with AXL-APTAMER + paclitaxel had significantly fewer CD31^{+} cells than the mice treated with control aptamer + paclitaxel. Overall, the results from two different OC animal models indicate that the AXL-APTAMER alone is effective in reducing the tube formation in the HeyA8 model and paclitaxel combination with AXL-APTAMER results in enhanced inhibition of angiogenesis in SKOV3-IP1, suggesting that the inhibition of AXL reduces the angiogenesis process.

DISCUSSION

In the current study, we demonstrated that AXL receptor tyrosine kinase (RTK) is associated with significantly shorter OC survival and its inhibition by highly specific chemically modified serum stable AXL-APTAMERs suppresses tumor growth and intraperitoneal metastasis in OC tumor models. AXL-APTAMER also showed an inhibitory effect on cancer cell proliferation, invasion/metastatis, and angiogenesis, contributing to the in vivo antitumor efficacy of the highly specific treatment. Targeting AXL by the aptamers also enhanced the efficacy of chemotherapy (paclitaxel, a first-line chemotherapy agent in OC) in the in vivo models.

Our finding that AXL overexpression is significantly associated with poor survival in patients with high-grade serous OC is consistent with previous reports indicating that AXL regulates tumor growth in some cancers, as well as reports showing that AXL activity is involved in the regulation of epithelial-to-mesenchymal transition and metastasis.[10,12,13,23] These data indicate AXL as a potentially useful therapeutic target in metastatic OC.

There have been some efforts to develop inhibitors for AXL-RTK via small non-coding RNAs and small molecule inhibitors.[32–34] Although small molecule inhibitors lead to increased therapeutic efficacy and sensitivity in targeting these kinases, they can inhibit additional kinases potentially leading to unexpected toxicities.[35] For instance, AXL inhibitor BGB324 has been shown to inactivate the increased cell proliferation, survival, and chemoresistance of acute myeloid leukemia cells.[24] AXL inhibitors based on small non-coding RNAs have also been shown to successfully reduce proliferation and metastasis of various cancer cells.[23,32,36–38] However, clinical development of RNAi-based therapeutics is hampered by the lack of nanodelivery systems that can efficiently and safely deliver these small molecules into tumors.[39] Aptamers have been shown to provide favorable specificity and stability in in vivo studies. The key features of the aptamers as therapeutics are that they can easily be modified to optimize their characteristic features, such as stability, affinity, and specificity. Nucleic acid aptamers have several advantages over other therapeutic options, including (1) high binding affinity[40,41] and (2) decreased sensitivity to endonucleases by chemical modifications, such as fluoro modifications on the 2′ moiety of the ribose and phosphorothioate modifications.[42–44] In this study, we used a previously characterized RNA aptamer (GL21.T), which is known to bind AXL tyrosine kinase receptor with high affinity,[45] as the base sequence to synthesize the corresponding DNA aptamer. Since RNA oligonucleotides are more susceptible to hydrolysis than their DNA counterparts and

Figure 4. AXL-APTAMER Treatment Inhibits Signaling Pathways Promoting Invasion and Metastasis in OC Cells

(A) Wound-healing assays were performed for SKOV3-IP1 cells using AXL-APTAMER, CTL aptamer (100 nM), and without any treatment. Inhibition of cell motility by AXL-APTAMER is evident at time 24 and 48 hr. The p values were obtained with Student's t test (*p < 0.05); error bars represent mean values ± SEM. (B) Cell migration assay was performed using AXL-APTAMER, CTL aptamer (100 nM), and without treatment for HeyA8 cells. Inhibition of HeyA8 cell motility by AXL-APTAMER is evident at time 12 and 20 hr. The p values were obtained with Student's t test (*p < 0.05); error bars represent mean values ± SEM. (C) Invasion through matrigel toward 10% FBS was carried out in the presence of AXL-APTAMER or the control (unrelated) aptamer (400 nM) for 24 hr in SKOV3-IP1 (top) and HeyA8 (bottom) cell lines. (D) In vitro cell invasion was evaluated in matrigel Boyden chambers. Cells were quantitated by counting the cell number in at least four different fields per image. Data were analyzed as mean of cell number per field of view for two independent experiments with technical replicates per experiment; error bars represent mean values ± SD. (E) Immunoblotting for the proteins related to cell migration. matrix metalloproteinase 1 (MMP1) and MMP2, as well as p-FAK, were decreased upon AXL-APTAMER treatment (400 nM) for 48 hr. p-FAK and MMP2 were probed using the same membrane. Likewise, FAK and MMP1 were probed on the same membrane as well. Quantification of the bands was performed using ImageJ and represented by fold change values (*p < 0.05 and ****p < 0.0001).
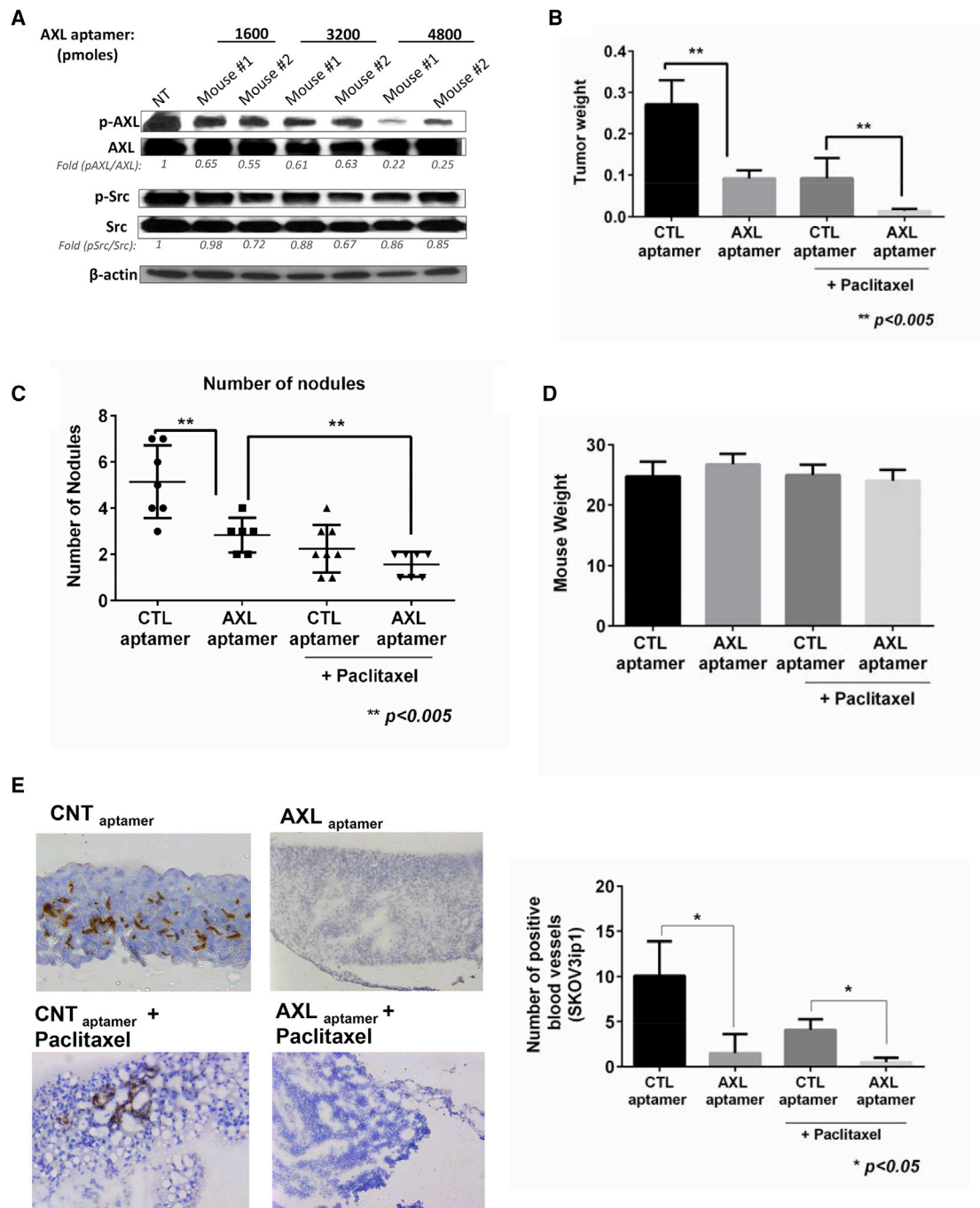
Figure 5. In Vivo Systemic i.v. Administration of AXL-APTAMER Inhibits Tumor Growth in the SKOV3-IP1 OC Model

(A) AXL-aptamer treatment inhibits pAXL and p-Src in HeyA8 tumors in mice. 4,800 pmole (1.8 mg/kg) was determined as the treatment dose for the following in vivo experiments. (B) AXL-APTAMER treatment (1.8 mg/kg) significantly reduces tumor weight compared to control aptamer in vivo in the SKOV3-IP1 orthotopic animal model (n = 10/per group). Combination with paclitaxel therapy resulted in a more dramatic decrease in tumor weight. (C) The number of intraperitoneal metastatic nodules was markedly reduced after AXL-APTAMER treatment in the SKOV3-IP1 animal model. (D) Non-significance in mouse weight between the groups indicates no toxicity in the SKOV3-IP1 animal model. (E) Immunohistochemistry analysis of angiogenesis marker (CD31) for CTL aptamer and AXL-APTAMER groups alone and in combination with chemotherapy for SKOV3-IP1. The p values were obtained with Student's t test (*p < 0.05 and **p < 0.001); error bars represent mean values ± SD.

Table 1. The Sequence of the Aptamers Used in the Study

Aptamer	Sequence	Modifications[a]	Denaturing
AXL aptamer (GLD-1)	5′-d(AUGAUCAAUCGCCUCAAUUCGA CAGGAGGCUCAC)-3′	2′-fluoro: on dC and dU monothio: on selected bases	85°C for 5 min, followed by incubation on ice for 2 min and at 37°C for 10 min
Control	5′-d(UUCGUACCGGGUAGGUUGGCUUGCA CAUAGAACGUGUCA)-3′	2′-fluoro: on dC and dU monothio: on selected bases	85°C for 5 min, followed by incubation on ice for 2 min and at 37°C for 10 min

[a]Chemical modifications (2′-fluro and monothio) are indicated by underline.

DNA aptamers are more cost effective in terms of synthesis compared to RNA aptamers,[46] in this study we synthesized and used a DNA aptamer with 2′-fluoro and monothiophosphate chemical modifications to further enhance the stability against endonucleases.

Our data show that application of 2′-fluoro and monothiophosphate modifications rendered the AXL-DNA-APTAMER stable for up to 24 hr in high concentrations of human serum, allowing the inhibition of AXL phosphorylation, hence, in turn, leading to strong, prolonged inhibition of downstream oncogenic signaling pathways, such as cancer metastasis and survival.

AXL has been further shown to be a downstream effector of the epithelial-to-mesenchymal transition, which promotes mobility, invasion, and metastasis.[12] In OC, AXL was shown to regulate cancer cell invasion and progression via altering MMPs and PI3K/AKT signaling.[23] Furthermore AXL inhibition led to the inhibition of FAK activity, which is one of the key regulatory mechanisms of the invasion pathway.[47] Overall, our data suggest that inhibition of FAK phosphorylation and MT1-MMP1 and MMP2 by the AXL aptamer is a key underlying mechanism of the inhibition of migration and invasion of OC cells.

We demonstrate that AXL-APTAMER treatment reduced the tumor burden and number of metastatic nodules in mice. When combined with paclitaxel, the AXL aptamer significantly enhanced antitumor efficacy of paclitaxel chemotherapy. Given the fact that AXL confers drug resistance in many cancers,[48–51] these results suggest that AXL-APTAMER not only provides additional antitumor effect but also, by inhibiting downstream signaling such as PI3K, ERK-MAPK, and nuclear factor κB (NF-κB), overcomes drug resistance in cancer cells. Therefore, AXL-APTAMER plus chemotherapy combinations may be a potential strategy for drug-resistant OC, and also it may serve as a tool for targeted delivery of chemotherapy to tumor while sparing healthy cells from chemotherapy-induced damage. Whether AXL-APTAMER conjugated to a chemotherapy agent provides efficient targeted therapy for OC patients can be proposed as a future scope of this study. Aptamer in combination with paclitaxel therapy opens up the possibility of conjugating the aptamer chemically to paclitaxel for more efficient and targeted therapy. Our data indicate AXL-APTAMER's potential as a therapeutic agent either alone or in combination with chemotherapy.

MATERIALS AND METHODS

Cell Lines

Human epithelial OC cell lines HeyA8 and SKOV3-IP1 were cultured in RPMI medium supplemented with 10% fetal bovine serum (FBS) and 100 IU/mL penicillin-streptomycin. All cells were maintained at 37°C with 5% CO_2 and 95% air and tested for mycoplasma using a MycoAlert mycoplasma detection kit (Lonza), as described by the manufacturer. All cell lines were obtained from the MD Anderson Characterized Cell Line Core Facility, which supplies authenticated cell lines, and all experiments were conducted when cells were 70%–80% confluent.

Aptamers

A GL21.T RNA aptamer 32 was used as the base sequence to generate a more stable DNA aptamer targeting the AXL oncoprotein. 2′-fluoro (on dC and dU) and monothio modifications were incorporated into AXL-APTAMER on selected bases. The sequences of the aptamers used in this study and their 5′-monothio modifications (underlined) are indicated in Table 1. Before each treatment, to promote the formation of ideal secondary structure, each aptamer was subjected to a denaturing step (85°C for 5 min, followed by incubation on ice for 2 min and at 37°C for 10 min) individually to promote the formation of ideal secondary structure.

Aptamer Synthesis

Aptamers were synthesized on an Expedite 8909 Oligo Synthesizer (Applied Biosystems,) using standard phosphoramidite chemistry.[52] Standard DNA synthesis reagents, Cy3-phosphoramidite, 5′-biotinTEG phosphoramidite, and Sulfurizing Reagent II were purchased from Glen Research. 2′-fluoro-dC and 2′-fluoro-dU phosphoramidites were purchased from both Glen Research and from Sigma-Aldrich. Aptamers were deprotected in concentrated ammonium hydroxide overnight at room temperature, vacuum dried overnight, and purified by reverse-phase chromatography over a Hamilton PRP-1 column on an AKTA 10 purifier (General Electric), by loading using a 100 mM triethylamine acetate buffer (pH 8.4) and eluting with increasing acetonitrile concentrations. Aptamer concentrations were determined using extinction coefficients estimated by OligoCalc.[53]

Filter-Binding Assay

Binding affinity of AXL-APTAMER to AXL-protein was determined by dual-membrane filter-binding assay. AXL-APTAMER

with biotin-TEG modification at the 5′ end for streptavidin-horseradish peroxidase (HRP) chemiluminescent detection was synthesized and purified as described above. Of 15 nM AXL-APTAMER, 1 μL was incubated with AXL-protein (2 to 2,000 nM, serial half-dilutions) in 3.5 μL 10 mM Tris-HCl (pH 7.4) (TE buffer) for 30 min at room temperature. After incubation, each reaction was diluted to 30 μL with TE buffer and filtered through a 96-well dot blot apparatus (Bio-Rad) with nitrocellulose layered on top of a nylon membrane. Nitrocellulose will retain protein-DNA complexes and the nylon membrane traps free DNA. The membranes were washed three times with 100 μL TE to wash away unbound DNA from the nitrocellulose membrane down to the nylon. Following washes, both membranes were UV cross-linked to immobilize the retained DNA, and they were processed for chemiluminescent detection using the Pierce biotinylated nucleic acid detection kit, according to the manufacturer's instructions. The chemiluminescent signals were detected and imaged on a Fluorochem imager (Alpha Innotech). Image analysis and quantification of spot intensities were conducted using ImageJ. Data from nylon membrane were used to calculate the fraction of DNA bound, and a binding curve was generated using GraphPad Prism software assuming a single binding site.

AXL-APTAMER Stability in Human Serum

To determine the stability of AXL-APTAMER, it was incubated in 80% human serum (4 μM) for periods ranging from 1 hr to 7 days. Type AB Human Serum was used (Euroclone ECS0219D). At each time point indicated, 4 μL serum (16 pmol DNA) was withdrawn and incubated for 1 hr at 37°C with 5 μL proteinase K solution (600 mAU/mL) to remove serum proteins that interfere with electrophoretic migration. Following proteinase K treatment, 18 μL denaturing gel loading buffer was added to each sample, and the samples were then stored at −80°C. Samples from each time point were separated by electrophoresis on 15% denaturing polyacrylamide gels. The gels were stained with ethidium bromide and visualized by UV light exposure.

Cell Viability Assay

The viability of cells was detected by MTS assay (Promega). Viable cells were seeded at a density of 1,250 cells/well in 96-well plates. The next day, cells were treated with the AXL-APTAMER or control aptamer for 24, 48, and 72 hr. At the end of the treatments, MTS and phenazinemethosulfate (PMS, 20:1 v/v) solutions were added to the cells, and the viability of growing cells was measured by monitoring the absorption of the product at 490 nm. All experiments were performed in six replicates, and the results were reported as the mean absorption ± SEM.

Immunofluorescence

SKOV3-IP1 OC cells were plated on six-well plates and treated with Cy3-labeled AXL-APTAMER. Following 3 hr of treatment, cells were washed with PBS and fixed with 4% paraformaldehyde. Nuclei were visualized by Hoechst counterstaining.

Invasion Assay

Cell invasiveness was assayed in a transwell system (24-well, 8-μm pore size; BD Falcon) according to the manufacturer's manual. Briefly, cells were treated with the AXL-APTAMER or control aptamer, and 3 hr later were suspended in serum-free medium (200 μL) and placed into the matrigel-coated upper chambers of the transwell insert (7.0×10^5/chamber). The lower chambers were filled with medium containing 10% FBS as the chemo-attractant. The chambers were incubated at 37°C in 5% CO_2 for 24 hr. After this incubation, the cells in the upper chambers were removed with cotton swabs, and the cells that had passed through the matrigel were fixed, stained, and counted by light microscopy.

In Vitro Cell Migration Assay

Cells were plated onto six-well plates ($8–10 \times 10^4$ cells/well) in duplicate in cell culture medium supplemented with 10% FBS and then cultured to confluence. After 24 hr, the cells were treated with AXL-APTAMER for 3 hr. A scratch was made in the surface of each culture with a 200-μL sterile micropipette tip. Cells were photographed at baseline (t = 0) and at regular intervals on a phase-contrast microscope (Nikon Instruments). The wound healing was assessed visually by comparing photographs taken at baseline with those taken 12 and 24 hr later.

Western Blotting

Cells were subjected to lysis with ice-cold radioimmunoprecipitation (RIPA) buffer, and protein concentration was determined by using the BCA Assay Kit (Thermo Scientific). Protein samples were separated on 4%–15% gradient polyacrylamide gels (Bio-Rad) and then electro-transferred onto polyvinylidene fluoride membranes (EMD Millipore). Membranes were blocked with 5% non-fat milk, rinsed, and incubated with primary antibodies against pAXL and AXL (R&D Systems). After overnight incubation at 4°C, membranes were washed and incubated with their corresponding secondary antibody. Signals were detected with an enhanced chemiluminescence detection kit (Denville Scientific). Immunoblots were scanned by an Alpha Imager densitometer (Alpha Innotech) for quantification of protein expression. Protein β-actin (Sigma-Aldrich) was used as a loading control.

In Vivo Experiments with OC Tumor Models

For in vivo experiments, 10- to 12-week-old female nude mice were obtained from the National Cancer Institute. All experiments were approved by the Institutional Animal Care and Use Committee of MD Anderson Cancer Center, where the experiments were carried out.

To determine effective in vivo dose of AXL-APTAMER, we first performed a dose-response experiment. HeyA8 cells (3×10^5 cells/ 0.2 mL Hank's balanced salt solution [HBSS]) were injected intraperitoneally into the mice to produce peritoneal tumors. Tumor growth was monitored visually. After 14–21 days, when tumor growth was confirmed visually, mice were injected intravenously with one of three different concentrations of AXL-APTAMER. Mice were killed 72 hr

after this injection. Tumor tissue extracted from each mouse was subjected to western blot analysis to quantify pAXL expression. Following the first in vivo dose-response experiment, another in vivo experiment was performed to test the antitumor activity of the AXL-APTAMER in OC.

To evaluate antitumor activity of AXL-APTAMER, we used two different models. In the HeyA8 intraperitoneal mice model, nude mice (n = 5) were inoculated intraperitoneally with HeyA8 cells (2.5×10^5 cells/0.2 mL HBSS) to generate tumors. Then 2 weeks later, after peritoneal tumor growth was confirmed visually, mice were treated with the following: (1) control scrambled aptamer, (2) AXL-APTAMER alone, (3) paclitaxel alone, (4) control aptamer + paclitaxel, or (5) AXL-APTAMER + paclitaxel. Aptamers were administered i.v. three times weekly, while paclitaxel was administered intraperitoneally once weekly. Then 4 weeks after the beginning of treatment, mice were killed and tumors in the peritoneal cavity were excised and weighed.

In the SKOV3-IP1 animal model, nude mice (n = 10) were inoculated intraperitoneally with SKOV3-IP1 cells (1×10^6 cells/0.2 mL HBSS) to generate tumors. Then 2 weeks later, after peritoneal tumor growth was confirmed visually, mice were treated with the following: (1) control scrambled aptamer, (2) AXL-APTAMER alone, (3) control aptamer + paclitaxel, or (4) AXL-APTAMER + paclitaxel. Aptamers were administered i.v. three times weekly, while paclitaxel was administered intraperitoneally once weekly. Then 5 weeks after the beginning of treatment, mice were killed and tumors in the peritoneal cavity were excised and weighed. For immunohistochemistry, tumors were fixed in formalin and embedded in paraffin and/or were embedded in optimum cutting temperature compound (Miles), rapidly frozen in liquid nitrogen, and stored at 80°C.

Immunohistochemistry

The immunohistochemical analysis was perfomed as previously described.[54] Briefly, unstained sections of mouse tumor tissue were deparaffinized and rehydrated. Antigens were retrieved by using Dako antigen retrieval solution. Endogenous peroxidase was blocked with 3% hydrogen peroxide. Primary antibodies against CD31 (Abcam) were incubated overnight at 4°C. The next day, a goat anti-rabbit horseradish peroxidase secondary antibody (Jackson ImmunoResearch Laboratories), diluted in blocking solution, was added and the samples were incubated for 1 hr at room temperature. Slides were developed with 3,3′-diaminobenzidine (DAB) substrate (Vector Laboratories) and counterstained with Gill no. 3 hematoxylin solution. To quantify CD31 expression, the positive (DAB-stained) cells were counted in five random fields per slide.

Statistical and Survival Analysis

Quantitative data for different groups were compared by the Student's t test, and p values < 0.05 were considered significant. The normality of the distribution was tested by using the Shapiro-Wilk test.

Survival analysis was performed in R (version 3.0.1) (https://www.r-project.org), and the statistical significance was defined as a p value less than 0.05. We downloaded RNASeqv2 Level3 data publicly available from TCGA (https://gdc.cancer.gov) for AXL in patients with ovarian serous cystadenocarcinoma (OV). Patient overall survival information was retrieved from cbioPortal (http://www.cbioportal.org). We ended up with complete information for 303 patients. We performed Cox regression analysis for associations between survival and AXL mRNA levels. The analysis yielded a hazard ratio of 1.3 (95% confidence interval [CI] = [1.02, 1.68], Wald test p value = 0.03) for cases with high AXL (last tertile, 66–100th percentile of range) compared to cases with low AXL (first tertile, 0–33th percentile of range). The Kaplan-Meier plots were generated for this dichotomization. The numbers of patients at risk in low and high AXL groups at different time points are presented at the bottom of the graph. The median survival times for each group are shown in brackets.

SUPPLEMENTAL INFORMATION

Supplemental Information includes two figures and can be found with this article online at http://dx.doi.org/10.1016/j.omtn.2017.06.023.

AUTHOR CONTRIBUTIONS

P.K. designed, conducted, interpreted, and analyzed both in vitro and in vivo studies. B.O. helped in the interpretation of all the studies conducted. B.A. helped in the design and conduct of the animal studies. R.B. helped with conducting in vitro experiments and participated in the interpretation of the results. N.G. assisted in the initial aptamer in vitro experiments. C.R.-A. helped in the design and conduct of the animal study. E.B. participated in animal studies. M.D. assisted in in vitro experiments. V.G.-V. assisted in immunohistochemistry (IHC) study. C.I. conducted the analysis of TCGA and animal models. G.L.R.L. synthesized the aptamer and helped with the filter-binding experiment. P.A. assisted with the filter-binding experiment. S.C. helped with the stability experiment. M.H. and S.Y.-Y.W. participated in take-down of the animal studies. R.M. helped in the interpretation of the results. D.G.G., D.E.V., and V.d.F. helped in overall design and interpretation of in vitro data. A.K.S. helped in the overall design, conduct, analysis, and interpretation of animal models. G.L.-B. directed, designed, analyzed, and interpreted all of the experiments conducted in the study. P.K., R.M., B.O., and G.L.-B. prepared and corrected all versions of the manuscript and all elements related to this body of work. All authors edited and approved the final manuscript.

CONFLICTS OF INTEREST

D.G.G. has a financial interest in AM Biotechnologies, Inc.

ACKNOWLEDGMENTS

REFERENCES

1. Siegel, R.L., Miller, K.D., and Jemal, A. (2015). Cancer statistics, 2015. CA Cancer J. Clin. 65, 5–29.

2. Gilks, C.B., and Prat, J. (2009). Ovarian carcinoma pathology and genetics: recent advances. Hum. Pathol. 40, 1213–1223.

3. Raja, F.A., Chopra, N., and Ledermann, J.A. (2012). Optimal first-line treatment in ovarian cancer. Ann. Oncol. 23 (Suppl 10), x118–x127.

4. Kumar, S., Mahdi, H., Bryant, C., Shah, J.P., Garg, G., and Munkarah, A. (2010). Clinical trials and progress with paclitaxel in ovarian cancer. Int. J. Womens Health 2, 411–427.

5. Yang, D., Yu, L., and Van, S. (2010). Clinically relevant anticancer polymer Paclitaxel therapeutics. Cancers (Basel) 3, 17–42.

6. Zeimet, A.G., Reimer, D., Radl, A.C., Reinthaller, A., Schauer, C., Petru, E., Concin, N., Braun, S., and Marth, C. (2009). Pros and cons of intraperitoneal chemotherapy in the treatment of epithelial ovarian cancer. Anticancer Res. 29, 2803–2808.

7. Machida, S., Saga, Y., Takei, Y., Mizuno, I., Takayama, T., Kohno, T., Konno, R., Ohwada, M., and Suzuki, M. (2005). Inhibition of peritoneal dissemination of ovarian cancer by tyrosine kinase receptor inhibitor SU6668 (TSU-68). Int. J. Cancer 114, 224–229.

8. Matulonis, U.A., Berlin, S., Ivy, P., Tyburski, K., Krasner, C., Zarwan, C., Berkenblit, A., Campos, S., Horowitz, N., Cannistra, S.A., et al. (2009). Cediranib, an oral inhibitor of vascular endothelial growth factor receptor kinases, is an active drug in recurrent epithelial ovarian, fallopian tube, and peritoneal cancer. J. Clin. Oncol. 27, 5601–5606.

9. Friedlander, M., Hancock, K.C., Benigno, B., Rischin, D., Messing, M., Stringer, C.A., Hodge, J.P., Ma, B., Matthys, G., and Lager, J.J. (2008). Pazopanib (Gw786034) Is Active in Women with Advanced Epithelial Ovarian, Fallopian Tube and Peritoneal Cancers: Results of a Phase Ii Study. Ann. Oncol. 19 (Suppl 8), viii211.

10. Zhang, Y.-X., Knyazev, P.G., Cheburkin, Y.V., Sharma, K., Knyazev, Y.P., Orfi, L., Szabadkai, I., Daub, H., Kéri, G., and Ullrich, A. (2008). AXL is a potential target for therapeutic intervention in breast cancer progression. Cancer Res. 68, 1905–1915.

11. Sainaghi, P.P., Castello, L., Bergamasco, L., Galletti, M., Bellosta, P., and Avanzi, G.C. (2005). Gas6 induces proliferation in prostate carcinoma cell lines expressing the Axl receptor. J. Cell. Physiol. 204, 36–44.

12. Gjerdrum, C., Tiron, C., Høiby, T., Stefansson, I., Haugen, H., Sandal, T., Collett, K., Li, S., McCormack, E., Gjertsen, B.T., et al. (2010). Axl is an essential epithelial-to-mesenchymal transition-induced regulator of breast cancer metastasis and patient survival. Proc. Natl. Acad. Sci. USA 107, 1124–1129.

13. Li, Y., Ye, X., Tan, C., Hongo, J.A., Zha, J., Liu, J., Kallop, D., Ludlam, M.J., and Pei, L. (2009). Axl as a potential therapeutic target in cancer: role of Axl in tumor growth, metastasis and angiogenesis. Oncogene 28, 3442–3455.

14. Shieh, Y.S., Lai, C.Y., Kao, Y.R., Shiah, S.G., Chu, Y.W., Lee, H.S., and Wu, C.W. (2005). Expression of axl in lung adenocarcinoma and correlation with tumor progression. Neoplasia 7, 1058–1064.

15. Sun, W., Fujimoto, J., and Tamaya, T. (2004). Coexpression of Gas6/Axl in human ovarian cancers. Oncology 66, 450–457.

16. Koorstra, J.B.M., Karikari, C.A., Feldmann, G., Bisht, S., Rojas, P.L., Offerhaus, G.J., Alvarez, H., and Maitra, A. (2009). The Axl receptor tyrosine kinase confers an adverse prognostic influence in pancreatic cancer and represents a new therapeutic target. Cancer Biol. Ther. 8, 618–626.

17. Antony, J., Tan, T.Z., Kelly, Z., Low, J., Choolani, M., Recchi, C., Gabra, H., Thiery, J.P., and Huang, R.Y. (2016). The GAS6-AXL signaling network is a mesenchymal (Mes) molecular subtype-specific therapeutic target for ovarian cancer. Sci. Signal. 9, ra97.

18. Halmos, B., and Haura, E.B. (2016). New twists in the AXL(e) of tumor progression. Sci. Signal. 9, fs14.

19. Lozneanu, L., Pinciroli, P., Ciobanu, D.A., Carcangiu, M.L., Canevari, S., Tomassetti, A., and Căruntu, I.D. (2016). Computational and Immunohistochemical Analyses Highlight AXL as a Potential Prognostic Marker for Ovarian Cancer Patients. Anticancer Res. 36, 4155–4163.

20. Willis, S., Villalobos, V.M., Gevaert, O., Abramovitz, M., Williams, C., Sikic, B.I., and Leyland-Jones, B. (2016). Single Gene Prognostic Biomarkers in Ovarian Cancer: A Meta-Analysis. PLoS ONE 11, e0149183.

21. Rea, K., Pinciroli, P., Sensi, M., Alciato, F., Bisaro, B., Lozneanu, L., Raspagliesi, F., Centritto, F., Cabodi, S., Defilippi, P., et al. (2015). Novel Axl-driven signaling pathway and molecular signature characterize high-grade ovarian cancer patients with poor clinical outcome. Oncotarget 6, 30859–30875.

22. Chen, P.X., Li, Q.Y., and Yang, Z. (2013). Axl and prostasin are biomarkers for prognosis of ovarian adenocarcinoma. Ann. Diagn. Pathol. 17, 425–429.

23. Rankin, E.B., Fuh, K.C., Taylor, T.E., Krieg, A.J., Musser, M., Yuan, J., Wei, K., Kuo, C.J., Longacre, T.A., and Giaccia, A.J. (2010). AXL is an essential factor and therapeutic target for metastatic ovarian cancer. Cancer Res. 70, 7570–7579.

24. Ben-Batalla, I., Schultze, A., Wroblewski, M., Erdmann, R., Heuser, M., Waizenegger, J.S., Riecken, K., Binder, M., Schewe, D., Sawall, S., et al. (2013). Axl, a prognostic and therapeutic target in acute myeloid leukemia mediates paracrine crosstalk of leukemia cells with bone marrow stroma. Blood 122, 2443–2452.

25. Sinha, S., Boysen, J., Nelson, M., Secreto, C., Warner, S.L., Bearss, D.J., Lesnick, C., Shanafelt, T.D., Kay, N.E., and Ghosh, A.K. (2015). Targeted Axl Inhibition Primes Chronic Lymphocytic Leukemia B Cells to Apoptosis and Shows Synergistic/Additive Effects in Combination with BTK Inhibitors. Clin. Cancer Res. 21, 2115–2126.

26. Widakowich, C., de Castro, G., Jr., de Azambuja, E., Dinh, P., and Awada, A. (2007). Review: side effects of approved molecular targeted therapies in solid cancers. Oncologist 12, 1443–1455.

27. Frumovitz, M., and Sood, A.K. (2007). Vascular endothelial growth factor (VEGF) pathway as a therapeutic target in gynecologic malignancies. Gynecol. Oncol. 104, 768–778.

28. Glaysher, S., Bolton, L.M., Johnson, P., Atkey, N., Dyson, M., Torrance, C., and Cree, I.A. (2013). Targeting EGFR and PI3K pathways in ovarian cancer. Br. J. Cancer 109, 1786–1794.

29. Mabuchi, S., Kawase, C., Altomare, D.A., Morishige, K., Sawada, K., Hayashi, M., Tsujimoto, M., Yamoto, M., Klein-Szanto, A.J., Schilder, R.J., et al. (2009). mTOR is a promising therapeutic target both in cisplatin-sensitive and cisplatin-resistant clear cell carcinoma of the ovary. Clin. Cancer Res. 15, 5404–5413.

30. Yap, T.A., Yan, L., Patnaik, A., Fearen, I., Olmos, D., Papadopoulos, K., Baird, R.D., Delgado, L., Taylor, A., Lupinacci, L., et al. (2011). First-in-man clinical trial of the oral pan-AKT inhibitor MK-2206 in patients with advanced solid tumors. J. Clin. Oncol. 29, 4688–4695.

31. Zuker, M. (2003). Mfold web server for nucleic acid folding and hybridization prediction. Nucleic Acids Res. 31, 3406–3415.

32. Li, R., Shi, X., Ling, F., Wang, C., Liu, J., Wang, W., and Li, M. (2015). MiR-34a suppresses ovarian cancer proliferation and motility by targeting AXL. Tumour Biol. 36, 7277–7283.

33. Keating, A.K., Kim, G.K., Jones, A.E., Donson, A.M., Ware, K., Mulcahy, J.M., Salzberg, D.B., Foreman, N.K., Liang, X., Thorburn, A., and Graham, D.K. (2010). Inhibition of Mer and Axl receptor tyrosine kinases in astrocytoma cells leads to increased apoptosis and improved chemosensitivity. Mol. Cancer Ther. 9, 1298–1307.

34. Vouri, M., An, Q., Birt, M., Pilkington, G.J., and Hafizi, S. (2015). Small molecule inhibition of Axl receptor tyrosine kinase potently suppresses multiple malignant properties of glioma cells. Oncotarget 6, 16183–16197.

35. Mócsai, A., Kovács, L., and Gergely, P. (2014). What is the future of targeted therapy in rheumatology: biologics or small molecules? BMC Med. 12, 43.

36. Mudduluru, G., Ceppi, P., Kumarswamy, R., Scagliotti, G.V., Papotti, M., and Allgayer, H. (2011). Regulation of Axl receptor tyrosine kinase expression by miR-34a and miR-199a/b in solid cancer. Oncogene 30, 2888–2899.

37. May, C.D., Garnett, J., Ma, X., Landers, S.M., Ingram, D.R., Demicco, E.G., Al Sannaa, G.A., Vu, T., Han, L., Zhang, Y., et al. (2015). AXL is a potential therapeutic target in dedifferentiated and pleomorphic liposarcomas. BMC Cancer 15, 901.

38. Xu, J., Jia, L., Ma, H., Li, Y., Ma, Z., and Zhao, Y. (2014). Axl gene knockdown inhibits the metastasis properties of hepatocellular carcinoma via PI3K/Akt-PAK1 signal pathway. Tumour Biol. 35, 3809–3817.

39. Wittrup, A., and Lieberman, J. (2015). Knocking down disease: a progress report on siRNA therapeutics. Nat. Rev. Genet. 16, 543–552.

40. Cao, H.Y., Yuan, A.H., Chen, W., Shi, X.S., and Miao, Y. (2014). A DNA aptamer with high affinity and specificity for molecular recognition and targeting therapy of gastric cancer. BMC Cancer 14, 699.

41. Keefe, A.D., Pai, S., and Ellington, A. (2010). Aptamers as therapeutics. Nat. Rev. Drug Discov. 9, 537–550.

42. Wang, R.E., Wu, H., Niu, Y., and Cai, J. (2011). Improving the stability of aptamers by chemical modification. Curr. Med. Chem. 18, 4126–4138.

43. Stein, C.A., Subasinghe, C., Shinozuka, K., and Cohen, J.S. (1988). Physicochemical properties of phosphorothioate oligodeoxynucleotides. Nucleic Acids Res. 16, 3209–3221.

44. Bennett, C.F., and Swayze, E.E. (2010). RNA targeting therapeutics: molecular mechanisms of antisense oligonucleotides as a therapeutic platform. Annu. Rev. Pharmacol. Toxicol. 50, 259–293.

45. Cerchia, L., Esposito, C.L., Camorani, S., Rienzo, A., Stasio, L., Insabato, L., Affuso, A., and de Franciscis, V. (2012). Targeting Axl with an high-affinity inhibitory aptamer. Mol. Ther. 20, 2291–2303.

46. Orava, E.W., Cicmil, N., and Gariépy, J. (2010). Delivering cargoes into cancer cells using DNA aptamers targeting internalized surface portals. Biochim. Biophys. Acta 1798, 2190–2200.

47. Kwiatkowska, A., Kijewska, M., Lipko, M., Hibner, U., and Kaminska, B. (2011). Downregulation of Akt and FAK phosphorylation reduces invasion of glioblastoma cells by impairment of MT1-MMP shuttling to lamellipodia and downregulates MMPs expression. Biochim. Biophys. Acta 1813, 655–667.

48. Zhang, Z., Lee, J.C., Lin, L., Olivas, V., Au, V., LaFramboise, T., Abdel-Rahman, M., Wang, X., Levine, A.D., Rho, J.K., et al. (2012). Activation of the AXL kinase causes resistance to EGFR-targeted therapy in lung cancer. Nat. Genet. 44, 852–860.

49. Elkabets, M., Pazarentzos, E., Juric, D., Sheng, Q., Pelossof, R.A., Brook, S., Benzaken, A.O., Rodon, J., Morse, N., Yan, J.J., et al. (2015). AXL mediates resistance to PI3Kα inhibition by activating the EGFR/PKC/mTOR axis in head and neck and esophageal squamous cell carcinomas. Cancer Cell 27, 533–546.

50. Hong, C.C., Lay, J.D., Huang, J.S., Cheng, A.L., Tang, J.L., Lin, M.T., Lai, G.M., and Chuang, S.E. (2008). Receptor tyrosine kinase AXL is induced by chemotherapy drugs and overexpression of AXL confers drug resistance in acute myeloid leukemia. Cancer Lett. 268, 314–324.

51. Dufies, M., Jacquel, A., Belhacene, N., Robert, G., Cluzeau, T., Luciano, F., Cassuto, J.P., Raynaud, S., and Auberger, P. (2011). Mechanisms of AXL overexpression and function in Imatinib-resistant chronic myeloid leukemia cells. Oncotarget 2, 874–885.

52. Caruthers, M.H., Barone, A.D., Beaucage, S.L., Dodds, D.R., Fisher, E.F., McBride, L.J., Matteucci, M., Stabinsky, Z., and Tang, J.Y. (1987). Chemical synthesis of deoxyoligonucleotides by the phosphoramidite method. Methods Enzymol. 154, 287–313.

53. Kibbe, W.A. (2007). OligoCalc: an online oligonucleotide properties calculator. Nucleic Acids Res. 35, W43–46.

54. Kanlikilicer, P., Rashed, M.H., Bayraktar, R., Mitra, R., Ivan, C., Aslan, B., Zhang, X., Filant, J., Silva, A.M., Rodriguez-Aguayo, C., et al. (2016). Ubiquitous Release of Exosomal Tumor Suppressor miR-6126 from Ovarian Cancer Cells. Cancer Res. 76, 7194–7207.